Article

Not peer-reviewed version

Coastal Wave Modeling and Forecasting with LSTM Optimization For Sustainable Energy Harvesting

Zaharaddeeen Karami Lawal * , Hayati Yassin * , Daphne Teck Ching Lai , Azam Che Idris

Posted Date: 18 May 2023

doi: 10.20944/preprints202304.0282.v2

Keywords: Numerical methods; Hyperparameters optimization; Ocean energy; Sustainable Energy; Recurrent neural network (RNN); Time series forecasting; Sustainability and environmental man-agement

Article

Coastal Wave Modeling and Forecasting with LSTM Optimization for Sustainable Energy Harversting

Zaharaddeeen Karami Lawal [1,4,*], Hayati Yassin [1,2,*], Daphne Teck Ching Lai [2,3] and Azam Che Idris [1]

[1] Faculty of Integrated Technologies, Universiti Brunei Darussalam, Gadong BE1410, Brunei; azam.che@gmail.com (A.C.I.)
[2] School of Digital Science, Universiti Brunei Darussalam, Gadong BE1410, Brunei; daphne.lai@ubd.edu.bn
[3] Institute of Applied Data Analytics (IADA), Universiti Brunei Darussalam, Gadong BE1410, Brunei
[4] Department of Computer Science, Federal University Dutse, Jigawa State 720223, Nigeria
* Correspondence: 21h5103@ubd.edu.bn (Z.K.L.); hayati.yassin@ubd.edu.bn (H.Y.)

Abstract: Coastal wave modeling and forecasting are essential in oceanography, sustainable marine energy, and ocean engineering. Precise forecasting of wave speed and direction are crucial for offshore operations, marine energy, risk management, environmental management, coastal and sustainable maritime management. The coastline of Brunei Darussalam can generate between 15 and 126 Giga Watt of wave energy. In this experimental research, we used two numerical approaches, the finite difference, and spectral element methods, to model and simulate wave speed and direction. We calculated the mean error between numerical and analytical solutions. We proposed a novel, promising, univariate time series forecasting model by combining the Long Short-Term (LSTM) with KerasTuner hyperparameters tuning and optimization techniques. This method helps us to improve the accuracy and efficiency of time-series forecasting.. The experimental data was computed from high-precision Acoustic Doppler Current Profiler (ADCP) sensor data. This research is part of the preliminary feasibility analysis of wave energy production in Brunei Darussalam and net zero commitment for a sustainable environment. Seven independent forecast experiments were performed for wave speed and direction in degree and radian units for 1, 3, 6, 8, 10, 12, and 24 hours. Mean squared error (MSE) was adopted as a metric for both training and testing. The experimental results reveal that the wave speed forecast has the lowest MSE compared to direction, regardless of the unit of measure, but has a longer duration. In addition, the direction forecast in the degree unit has the lowest errors compared to the unit of radians; the latter has a longer running time than the former**.** The model has delivered optimal results throughout the experiments with minor training and test errors. We conducted a thorough evaluations on two benchmark time series datasets, which include the study dataset and air quality index dataset, to validate the performance of the proposed model with other models. The proposed model outperforms cutting-edge forecasting models, such as the conventional LSTM, ARIMA, and Prophet. The model has the slightest forecast error compared to the existing literature's result.

Keywords: numerical methods; hyperparameters optimization; ocean energy; sustainable energy; Recurrent neural network (RNN); time series forecasting; sustainability and environmental management

1. Introduction

Coastal wave modeling has improved significantly in recent decades, due to the emergence of artificial intelligence applications. However, they still have a long way to go. Such modeling has a wide range of applications in fishing, maritime transport, naval navigation, environmental research, risk management and sustainable energy [1,2]. The advancement of activities in both nearshore and offshore waters requires knowledge of the wave condition [3,4] and the need to develop state-of-art wave forecasting systems. The wave prediction models are essential for disaster prevention and preparedness, optimization of shipping routes, climate change awareness, and ocean power generation [5]. Many research work has been done in the domain of coastal wave modeling, and the researchers have made a great breakthrough in forecasting wave conditions. However, wave predictions are sometimes inaccurate.

The wave modeling is frequently applied to simulate the significant physical occurrence in the coastal area [6-7]. For modeling and forecasting wave conditions, there is a need to consider and understand features like direction, frequency, speed, timing of waves, pressure, and wave height (amplitude), among others, and the correlation between these features. Different approaches are employed for coastal wave modeling [8-10]. The three primary modeling methods used are physical, numerical, and composite. Numerical models (NM) refer to the usage of computer codes (commercial, open source, or home-produced software) [11], and physical models (PM) refer to the usage of laboratory models at a suitable scale (micro, small, medium, and large-scale models) to study the process of interest, while composite models (CM) refer to the combined and proportional use of physical and numerical models [12]. At this phase, the conventional method of forecasting waves by oceanographers is numerical models [6]. To solve complex equations, the numerical models use various oceanic features as inputs, such as direction, speed, height, temperature, and pressure.

The most commonly used models nowadays are Simulating Waves Nearshore (SWAN) [6-13], which the Delft University of Technology developed and introduced by Booij et al. in 1999 [14], and WaveWatch III (WW3) was introduced by Tolman et al. in 2009 [15]. WaveWatch III (WW3) is a third-generation wave model developed by National Oceanic and Atmospheric Administration (NOAA)/ National Centers for Environmental Prediction (NCEP) [16].

The advantages of physical simulation and data-driven techniques are combined in traditional numerical model forecasting techniques to produce high spatial and sequential resolution predictions [17-18]. However, it has substantial drawbacks in real-world offshore sector applications because the accuracy and time lag are not guaranteed. Additionally, the numerical model should be carefully considered as an operational application due to the high computational and maintenance expenses [19–21].

Machine learning techniques have increasingly incorporated ocean wave prediction due to their advantages in establishing nonlinear mapping relationships, which can significantly boost prediction accuracy [22]. By combining the correlations between wind and wind waves with the data produced by a numerical model, Song et al. [6] developed a hybrid method called ConvLSTM by coupling CNN with LSTM to improve the predictions of significant height. Berbić et al. [23] use two classification models, ANN, and support vector machine (SVM), for significant wave height prediction.

Barbara et al. [24] use artificial neural networks (ANN) to forecast wave reflection from coastal and harbor structures. Elbisy et al. [25] developed a model using SVM with a genetic algorithm to predict wave direction and height and compare it with a neural network. The findings of this study show that the SVM model (RBF kernel) is a suitable alternative to NN for predicting wave parameters.

Even though the use of AI in wave condition forecasting is becoming increasingly common [6], hyperparameter optimization and training instability are amongst the biggest challenges of time series forecasting. In most of the literature, we found in various academic databases for ocean wave characteristics forecast such as speed, direction, and wave height parameters; among others, one of their biggest limitations is the optimization hyperparameters which leads to building overfitted models or models with high forecast errors.

Forecasting wave speed and direction is critical in sustainable marine energy harvesting because of the significant impact of these elements [26]. In this study, we aimed to propose a novel univariate time series forecast that will solve the problems of optimization and training instability, and this can be achieved by combining LSTM with hyperparameter tuning and optimization techniques. Our proposed model performs better than the models used in the research carried out by [6], [23], and [25].

The efficiency of wave power generation, which uses the energy of ocean or sea waves to generate electricity, is highly dependent on the direction and speed of the waves [27]. The direction of the waves can be used to determine the orientation of wave energy converters or wave farms, and the waves' speed impacts the amount of energy that can be generated [28,29]. By means of forecasting the speed and direction of sea waves, wave energy devices can be placed and operated to maximize their ability to generate energy [1, 30]. Additionally, precise wave direction and speed forecasts can reduce the risk of damage to infrastructure and ensure worker safety when using wave energy [29–31] Although wave energy harvesting technologies now exist at coastal sites, wave farms can have significant capital costs [29], making forecasting the energy generated in advance critical.

As part of Brunei Darussalam's vision for 2035 and energy transition, the country plans to harness vast marine energy from the South China Sea and fulfill its net zero commitment to a sustainable environment. According to Brunei Darussalam 2012 report prepared by the United Nations Climate Technology Centre and Network (UNCTCN). Approximately 269 km of Brunei Darussalam's coastline has the capacity to generate between 15 and 126 GW of wave energy, with an annual theoretical potential of 66 x 1010 W [32]. This study aims to conduct a preliminary efficiency and feasibility assessment of wave energy harvesting in Brunei Darussalam waters in the South China Sea. This research will help Brunei government achieve one of the sustainable development goals of affordable and clean energy.

The major objectives of this experiment are as follows:

- To simulate wave conditions using numerical schemes.
- To compute the mean error by comparing the difference between numerical and analytical solutions for each simulation.
- To propose a time series forecasting model capable of forecasting dynamic ocean conditions, and sustainable coastal and maritime operations using a hybrid method that combines LSTM with advanced hyperparameters tuning and optimization techniques.
- To validate the proposed model by comparing its performance with other models and datasets.

The rest of the paper is organized as follows: Section 2 describes the research area and the data used throughout the study. Section 3 presents the materials and methods of the study. With a discussion, Section 4 demonstrates and evaluates the results of the experiments. Section 5 presents a plan for future studies, while Section 6 summarizes the study.

2. Study Area and Data

Data for this experiment was computed using a high-precision underwater Acoustic Doppler Current Profiler (ADCP) sensor data collected in the territorial waters of Brunei Darussalam. Along the South China Sea coast at coordinates GPS (05 06.988 N, 114 59.833 E), procured by Universiti Brunei Darussalam for research purposes. The raw data collected by the sensor consists of many wave condition parameters, including temperature, pressure, significant wave height (Hm0), frequency, and current speed, and direction of different depths. Initially, professional divers placed the ADCP sensor on the seabed for data collection. Later, the sensor was retaken, and the raw data was retrieved using AquaPro. This software can also be used to monitor the wave condition captured by the sensor in real-time. The raw data file can be obtained by connecting the ADCP sensor with AquaPro. The raw data file was then uploaded to Storm64 for data visualization and preprocessing. The processed wave elements datasets can be generated at this stage and exported in different file formats like csv, txt, Whr, etc. AquaPro and Storm64 are developed by the sensor manufacturer Nortek Group, Australia. The exported preprocessed dataset underwent a data cleaning process before use. The wave speed and direction were estimated using the processed data collected from the sensor.

Preprints (www.preprints.org) | NOT PEER-REVIEWED | Posted: 18 May 2023 doi:10.20944/preprints202304.0282.v2

Figure 1. Google map indicating the location of the ADCP sensor on the South China Sea.

3. Materials and Methods

The methodology in this experiment consists of two parts. The first subsection is the wave speed and direction simulation using numerical methods for modeling and simulation. In contrast, the second subsections contain the details of univariate time series optimization and forecast using KerasTuner with long-short term memory (LSTM).

3.1. Numerical Modelling and Simulation

Numerical methods are mathematical techniques used to approximate solutions to problems that are difficult or impossible to solve analytically [33–35]. One such problem is wave speed and direction simulation, which can be approximated using the finite difference method and the Fourier transform. We used arbitrary values (sample data) in each simulation to simulate the wave speed and direction using the numerical method and compare them with analytical solutions [36,37].

In numerical modeling, the continuous values are converted into a discretized form. Discretization approximates a continuous function or system by a discrete set of points or values [33,38]. This process is commonly used in numerical methods such as the finite difference method and the Fourier transform. Below is a brief explanation of the two numerical approaches used in this study to simulate wave speed and direction.

3.1.1. Finite Difference Method

The finite difference method is a numerical method that discretizes a continuous function or system by dividing it into a finite number of points or nodes [39]. The function values at surrounding points then approximate the function values at each point. This approximation is based on a finite difference formula that connects the function's values at surrounding places to its derivative [40]. It is a widely used scheme for solving differential equations and is mainly suitable for problems comprising asymmetrical domains or boundary conditions.

This study used a one-dimensional finite difference approximation method to model the wave speed. The centered difference approach was used for analyzing the wave equation. The centered difference technique approximates the derivative as the slope of a line that passes through two points, which mitigates the influence of numerical errors caused by utilizing only one point, making it more accurate than the forward and backward difference methods.

Wave speed can be expressed as:

$$v = \frac{\lambda}{T} \quad (1)$$

Where v is the wave speed, λ is wavelength, and T is the period.

The first-order wave equation:

$$\frac{\partial u}{\partial t} + c\frac{\partial y}{\partial x} = 0,\ \ u(x, 0) = u_0\,(x) \quad (2)$$

Wave equation in one dimension (1D):

$$\frac{\partial^2 u}{\partial t^2} = c^2\frac{\partial^2 u}{\partial x^2} \quad (3)$$

Initial condition:

$$u(0, x) = u_0(x)\ \text{ and }\ u_t(0, x) = v_0(x)$$

Where c represents wave the speed, x represents space, and t represents time a function that describes how much the sea wave is displaced (amplitude) from its initial position at a particular point (x) and time (t) due to the wave passing through it, and v_0 represents the speed.

3.1.2. Fourier Transform

On the other hand, a function or signal can be converted from the time domain to the frequency domain using the Fourier transform [41]. Through this transformation, the frequency components of a signal can be examined and employed for tasks like filtering or smoothing. The Fourier transform is a continuous function [34–38].

It is usually calculated using a discrete algorithm, such as the fast Fourier transform (FFT), which approximates the transform at a finite number of discrete frequencies.

The Fourier transform function can be expressed as:

$$f(\omega) = \int_{-\infty}^{+\infty} f(t)e^{-(i\omega t)dt} \quad (4)$$

Where F(ω) is the Fourier transform of f(t) with respect to the frequency ω, i is the imaginary number (i.e., ($\sqrt{(-1)}$), ω is the angular frequency in radians per unit time $e^{-(}i\omega t)$ is the complex exponential function. We used a fast Fourier transform to implement the numerical solution of the wave direction. To calculate the directional spectrum, we applied the Pierson-Moskowitz spectrum equation.

Which can be expressed as:

$$S(f) = \alpha g^2(2\pi)^{-4}f^{-5}\exp\left(-\frac{5}{4}\left(\frac{f_m}{f}\right)^4\right) \quad (5)$$

3.2. Univariate Time Series Forecast

Univariate time series forecasting is the process of forecasting future values of a single variable over a period of time. This type of forecasting is commonly used in several fields, such as engineering, economics, and finance. This experiment focuses on the wave speed and direction of a specific location within the territorial waters of Brunei Darussalam. This study proposes a univariate time series approach to forecast wave speed and direction using LSTM recurrent neural network using the Python programming language. In this experiment, we used the stacking method to stack two layers of LSTM, two dense activation layers for relu and sigmoid, and one output dense layer. Stochastic gradient descent (SGD) optimizer was used for optimization, while Mean Squared Error (MSE) was chosen as a metric in both training and testing. In each hour, the sensor measured speed, direction, and other parameters five times, which means that each hour has 5 data points.

The dataset consists of 4925 rows and three columns for Date-Time, Direction, and Speed. Since we are conducting univariate time series forecast, we extracted separate datasets for direction and speed from the primary dataset by creating a data frame for each separately with DateTime as an index. The unit of direction measured is in degrees. We performed seven independent experiments for direction forecast for the next 1, 3, 6, 8, 10, 12, and 24 hours separately. We also converted the direction values from degrees to radians and ran another set of experiments using the same hours as in degrees. Furthermore, we run seven independent forecast experiments for speed using the same algorithm and hours as in the previous experiments. KerasTuner was used for hyperparameter tuning throughout the experiments, and the batch size was 32 for each experiment. During the

Preprints (www.preprints.org) | NOT PEER-REVIEWED | Posted: 18 May 2023 doi:10.20944/preprints202304.0282.v2

experiments, the sliding window size changes for each experiment, so we run seven experiment for each session.

The dataset was shuffled for every 1000 data points and divided into training and test sets throughout the experiments, making the models learn ideally and reducing the prediction's error to a minimal level. The training and validation set contains 3700, while the test set takes the remaining part. Each experiment was run as a single project because the Keras tuner saved the best model with hyperparameters for deployment or used later in JSON format and other folders like logs, etc. The maximum trial of each run is 2, and in each trial, the Keras tuner will find the best model, and at the end of the last trial execution, it will display the model with the lowest mean squared error (MSE) as the best model. The time elapsed will also be displayed.

TensorBoard was employed to display the learning curve. Typically, the KerasTuner saves the loss chart log history in a designated folder inside the project's main folder. After displaying the learning curve, the next is to test the best-trained model with the lowest MSE using the test set. We used the best model with the least MSE and made forecasts. Using the test set, we evaluated the MSE between the predicted and actual values. This study used NVIDIA GeForce GTX 1660 SUPER in terms of hardware CUDA Core 1408, RAM 64 GB, memory interface 192-bit, and a memory data rate of 14.00Gbps. Regarding the software, Jupyter Notebook with Keras 10.5 and Windows 10 was used in this experiment.

We used this research dataset, and made a forecast with other time series techniques. This comparative analysis will enable us to validate the performance of the newly proposed model. The time-series models we employ for the comparative study include ARIMA, Prophet, and the conventional LSTM. We also used the air quality index dataset and compared the performance of the proposed model with other models.

3.3. Long Short-Term Memory (LSTM)

Long short-term memory (LSTM) is a particular type of recurrent neural network (RNN), a broad name for a group of neural networks that can process sequential inputs. Hochreiter and Jürgen Schmidhuber first proposed RNN in 1997 [6, 42]. LSTM neural networks can handle some problems that need a long period because they employ "gates" to manage the memory process [43][44]. When learning long-term dependencies, recurrent neural networks encounter challenges such as bursting or vanishing gradients. LSTM was explicitly developed to deal with these issues. Vanilla LSTM consists of a cell, an input gate, and an output gate, a well-composed fundamental LSTM structure [45]. Later, Gers et al. [46] invented the forget gate, which can remove memory blocks whenever their information becomes worthless. The introduction of three gates in LSTM makes it different from RNN in most ways [47]. Careful regulation of the gate structure is required for the LSTM to add or remove information from nodes to change the information flow state [6, 48]. Figure 10 demonstrates the fundamental LSTM.

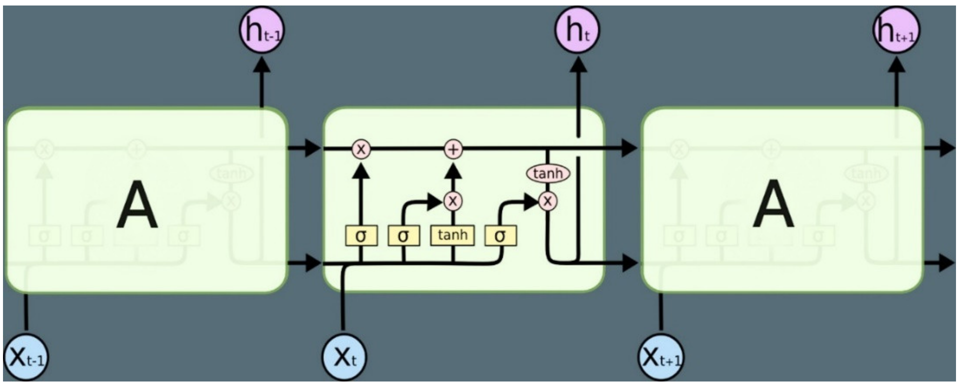

Figure 2. An LSTM's sequence component consists of four interacting layers.

An LSTM is typically comprised of the following gates:

Input gate: After the data is imported, the information must first pass through the input gate. Depending on the state of the cell, the switch selects whether or not to store the information. The input gate consists of two steps. First, the sigmoid layer selects which data needs to be updated. Second, the tanh layer generates new data X_t. They can be included in the state of the cell [43,49,50].

Output gate: The output gate determines how much information can be output. First, the sigmoid layer generates an initial output by scaling X_t with tanh to [–1,1]. Finally, the output of the model can be generated by multiplying the sigmoid output pair by pair [43,49].

Forgot gate: The sigmoid in the forget gate is in charge of controlling this. According to a ft value, which ranges between 0 and 1, it determines whether to allow the information collected (X_{t-1}) to flow. An LSTM layer exists in the LSTM neural network. The surrounding neurons in the same layer are also affected along with the output layer [43,51].

3.3.1. LSTM in Univariate Time Series Forecasting

Long Short-Term Memory (LSTM) is a form of recurrent neural network (RNN) designed to process sequential input, such as time series. LSTM is powerful and successful in univariate time series forecasting, outperforming standard statistical methods such as ARIMA and exponential smoothing in many scenarios [43,49–51].

The successful performance of LSTM in univariate time series forecasting is due to its capacity to identify complex patterns and correlations in the data [50]. In contrast to conventional modeling techniques, LSTM may detect long-term and non-linear dependencies in the data. It is, therefore, perfect for modeling time series data with trends, seasonality, and other intricate patterns [47,48].

Numerous applications, including financial, energy demand, and weather forecasting, have shown that LSTM is effective for univariate time series forecasting.

3.4. Evaluation Metrics

A widely popular evaluation metric, Mean Square Error (MSE), is used to evaluate models. MSE evaluates the mean squared deviation between the predicted and actual data value and averages it across the entire train or test dataset since MSE can be used in both situations [52]. The value of MSE is always positive since it is always taking the square of error. The following equation define the MSE:

$$\mathrm{MSE} = \frac{1}{N}\sum_{i=1}^{N}(y_i - \hat{y}_i)^2 \quad (6)$$

Where N represents the population or number of data points, y_i is the actual values, and $\hat{y}_i$ is the predicted values. The MSE is excellent for assuring that our trained model does not contain outlier predictions with significant errors since it gives more weight to these errors thanks to the squaring component of the function. However, in many practical situations, we do not worry about such outliers and instead seek a balanced model that performs satisfactorily on the majority

4. Result and Discussion

This study's experiment is based on wave speed, direction modeling, and forecasting using a numerical method and artificial intelligence techniques. We used two numerical methods, finite difference, and spectral element methods, to simulate wave speed and direction and compare the result with analytical solutions using Python codes. In the second part, we used LSTM stacking to forecast wave speed and direction in two units of measurement.

4.1. Wave Speed Simulation Using Centered Finite Difference Method

In this simulation, we model an ocean wave speed propagating along a one dimensional of the ocean surface using the centered difference method.

We first sets up a grid of points on the ocean surface with a total of points (n_x = length(x)) and a total of time steps (n_t = len(t)). The wave is transcribed off as by its amplitude A, and its wavelength k and frequency f are calculated from these parameters.

The initial condition of the wave is set to be a sinusoidal wave of amplitude A, and the wave equation is solved numerically for each time step using the centered difference method.

Preprints (www.preprints.org) | NOT PEER-REVIEWED | Posted: 18 May 2023 doi:10.20944/preprints202304.0282.v2

The mean error between the numerical and the analytical solution is calculated and displayed as shown in Figure 3.

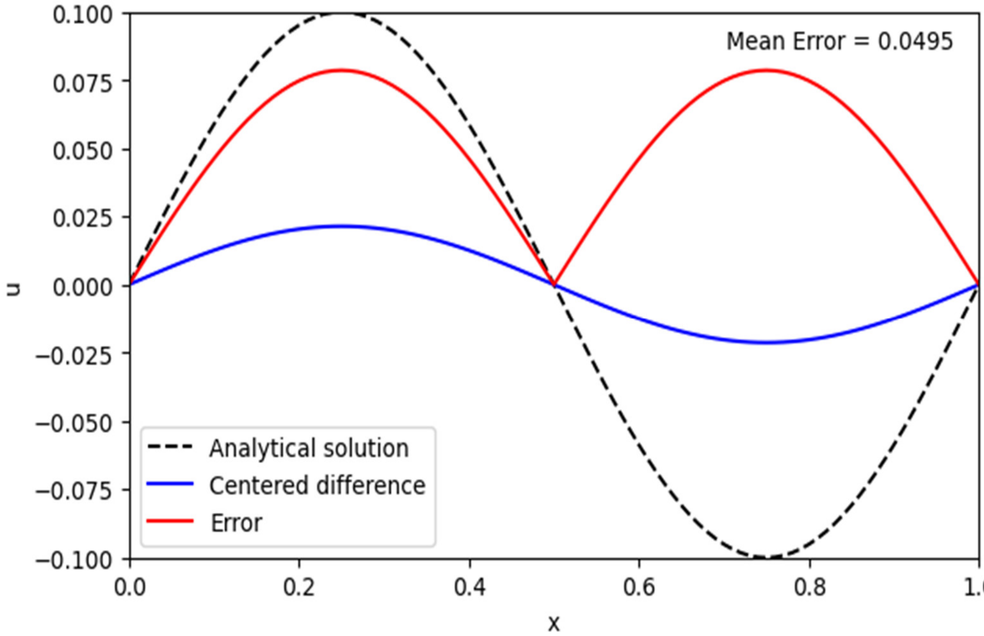

Figure 3. Wave speed simulation.

4.2. Wave Direction Simulation Using Fast Fourier Transformation

In this simulation, sample wave data is generated initially by combining two sinusoidal waves. The fftpack.fft() function from the scipy package is then used to calculate the Fourier transform of the wave data. We may determine the power spectrum by squaring the absolute value of the Fourier coefficients in each dimension.

To calculate the directional wave spectrum, we first define a set of angles (theta) and initialize an array for the directional spectrum. We then loop over each angle and calculate the directional spectrum using the equation 5 above.

In order to determine the mean wave direction, we used analytical and numerical solutions. The analytical method ascertain the power spectrum's angle of maximum power. The directional spectrum's highest value's angle is determined numerically. Then the results are plotted as shown in Figure 4.

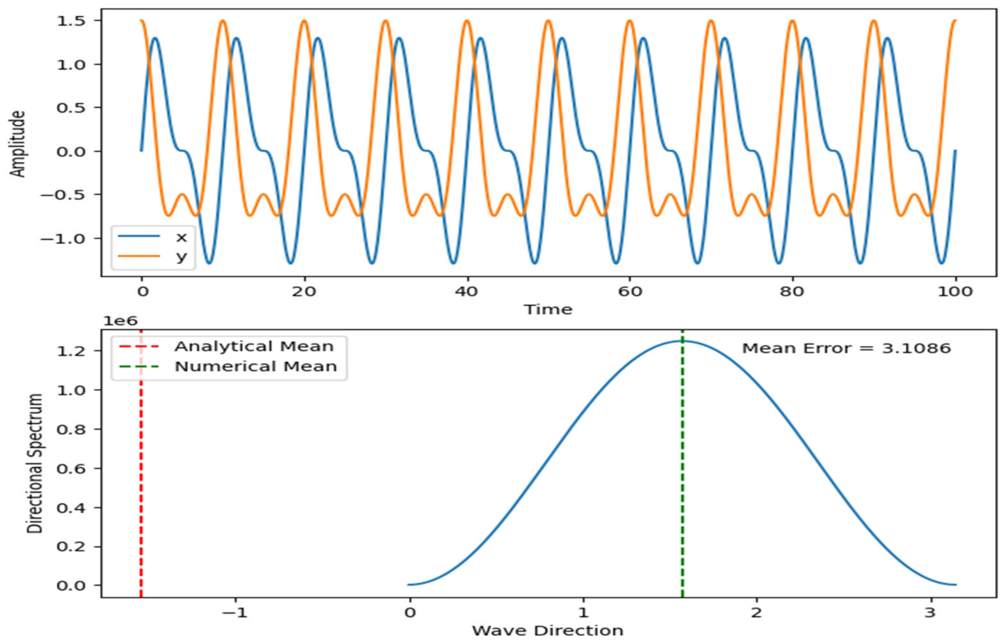

Figure 4. Wave direction simulation.

4.3. Wave Condition Forecasting with LSTM

This study's experiment is based on the wave direction and speed forecast, which consists of 4925 data points. Initially, the model training and validation were performed using a Keras tuner. The epoch versus loss and metric (mean squared error) graph was plotted using Tensorboard for each forecast experiment. The best model was tested with the test dataset, and the mean squared error was measured for each forecast experiment. The results of the experiment will be discussed in detail in this section.

4.3.1. Wave Direction Forecast (Degree)

In this experiment, wave direction forecasts were performed using degree and radian units. The main essence of running two wave direction forecasts in two different units of measurement is to identify the unit that can fit our model very well with minor prediction errors. This subsection will discuss and analyze the wave direction forecast in degree units. Figure 12 below illustrate the learning curve of wave direction forecasts.

Table 1 contains the experimental results. The forecast of wave direction (degrees) for the next 10 hours has the lowest MSE for training and testing. In contrast, the prediction for the next 1 hour has the highest MSE for training and testing. The predictions for the next 3 and 6 hours also have low training and test errors. Epoch loss decreased to zero at some point in both the first and second trials as shown in Figure 5.

Table 1. Direction Forecast (Degree).

Direction (Degree) Forecast					
Forecast Hours	Training MSE	Test MSE	No. of Epoch	Max. trial	Elapsed Time
1	0.0234	0.0302	100	2	18m 36s
3	0.0185	0.0261	1000	2	01h 01m 09s
6	0.0185	0.0245	1000	2	50m 42s
8	0.0196	0.0253	1000	2	01h 18m 38s
10	0.0183	0.0238	1000	2	01h 41m 30s
12	0.0198	0.0244	1000	2	02h 24m 09s
24	0.0197	0.0271	1000	2	03h 25m 50s

Preprints (www.preprints.org) | NOT PEER-REVIEWED | Posted: 18 May 2023 doi:10.20944/preprints202304.0282.v2

Figure 6 illustrates the training and test MSEs result in form of bar chart, and as expected, the test values are higher than the training values. The model is familiar with the training dataset and knows nothing about the test dataset. That is why the mean squared errors of the test are higher when compared to that of training. The average errors from 7 experiments for training and testing are 0.019 and 0.0259, respectively.

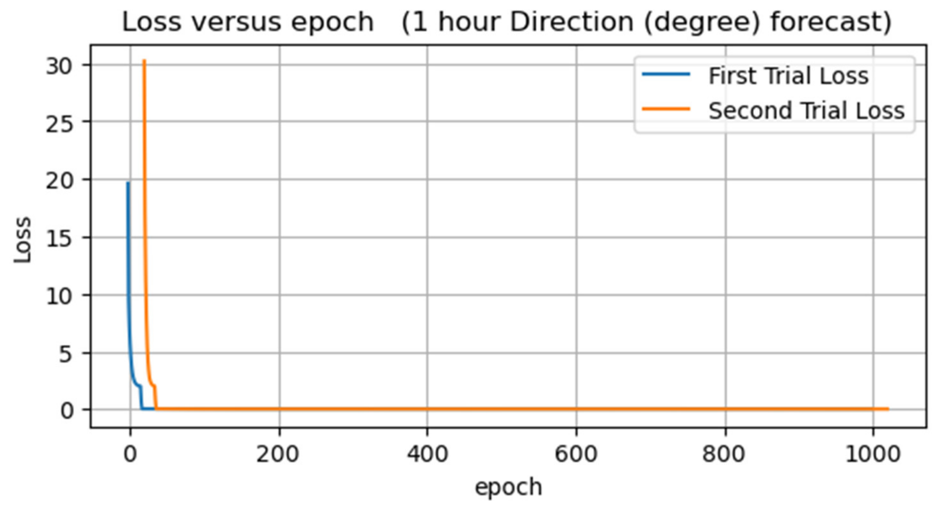

(**a**) Direction (degree) 1 hour forecast

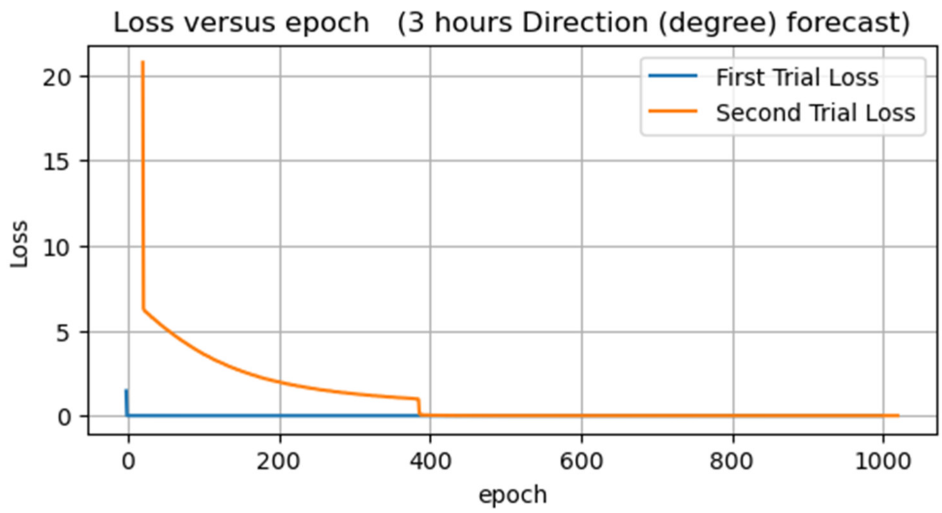

(**b**) Direction (degree) 3 hours forecast.

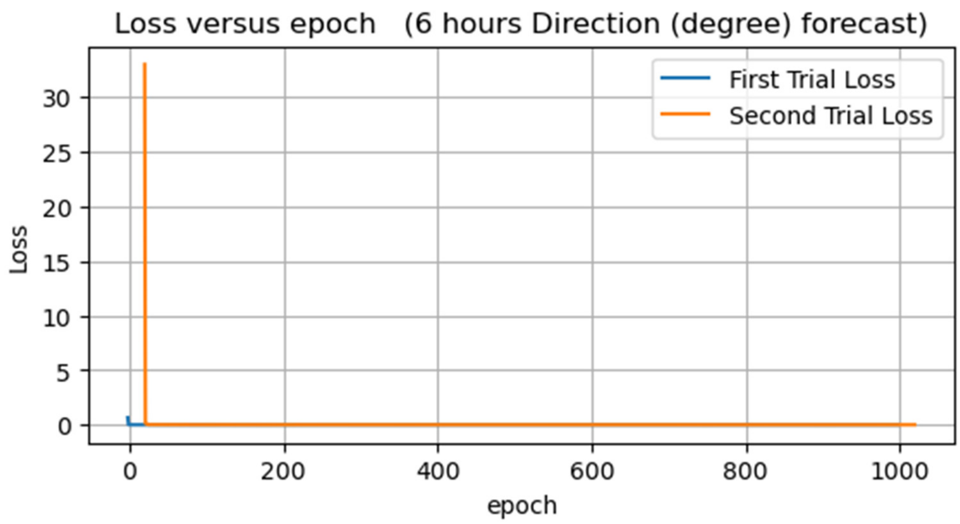

Preprints (www.preprints.org) | NOT PEER-REVIEWED | Posted: 18 May 2023 doi:10.20944/preprints202304.0282.v2

(**c**) Direction (degree) 6 hours forecast.

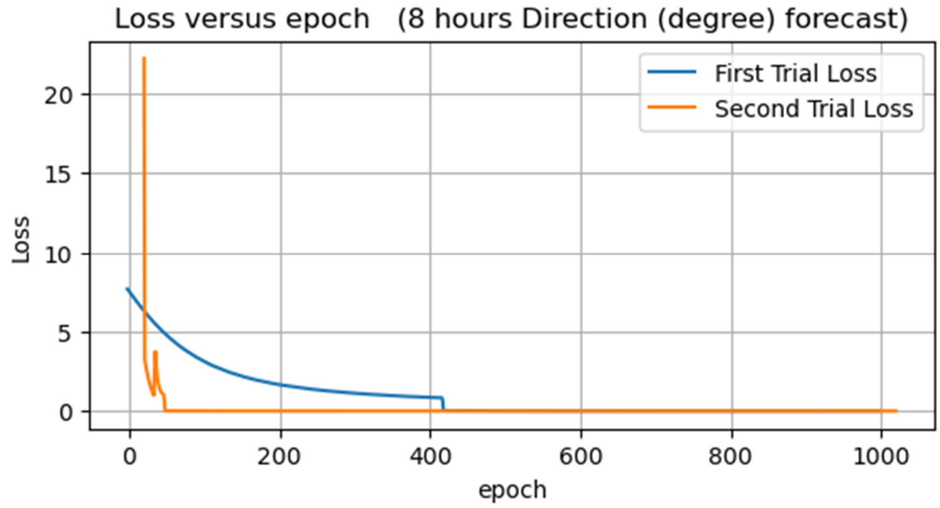

(**d**) Direction (degree) 8 hours forecast.

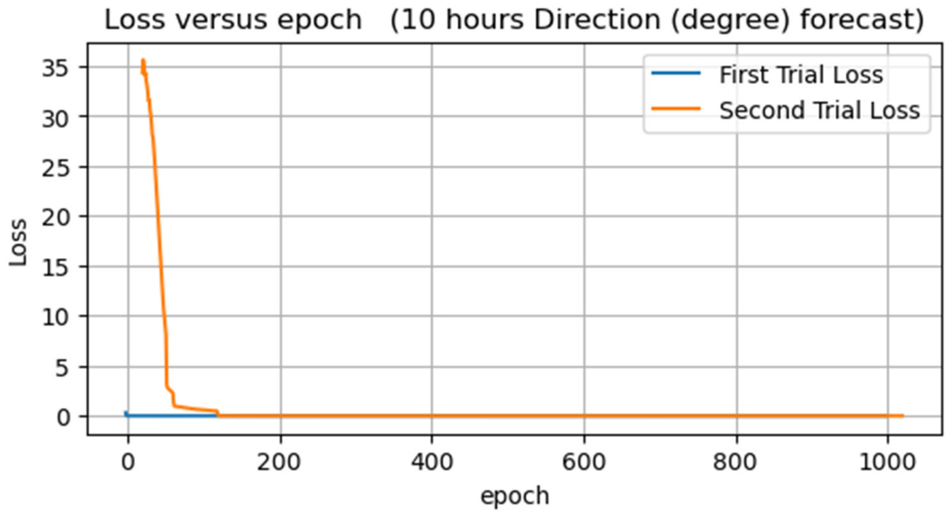

(**e**) Direction (degree) 10 hours forecast.

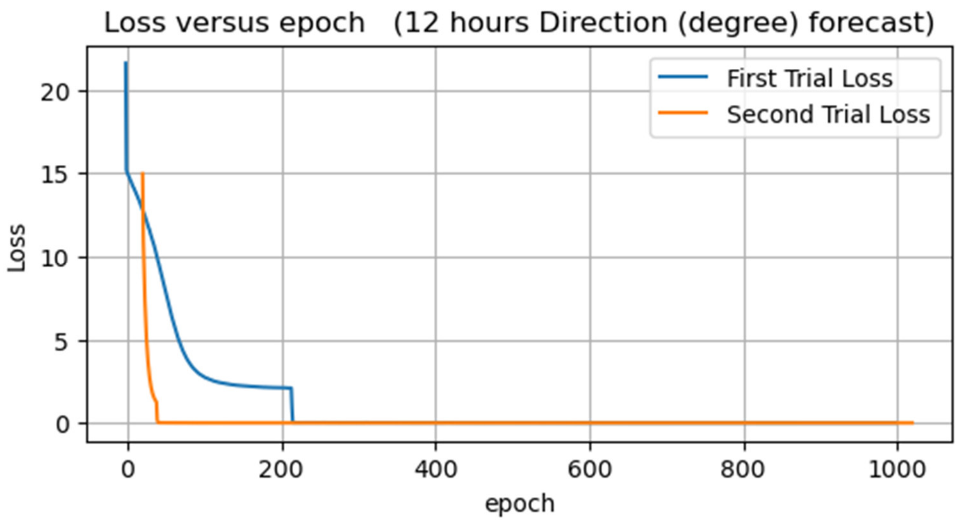

(**f**) Direction (degree) 12 hours forecast.

Preprints (www.preprints.org) | NOT PEER-REVIEWED | Posted: 18 May 2023 doi:10.20944/preprints202304.0282.v2

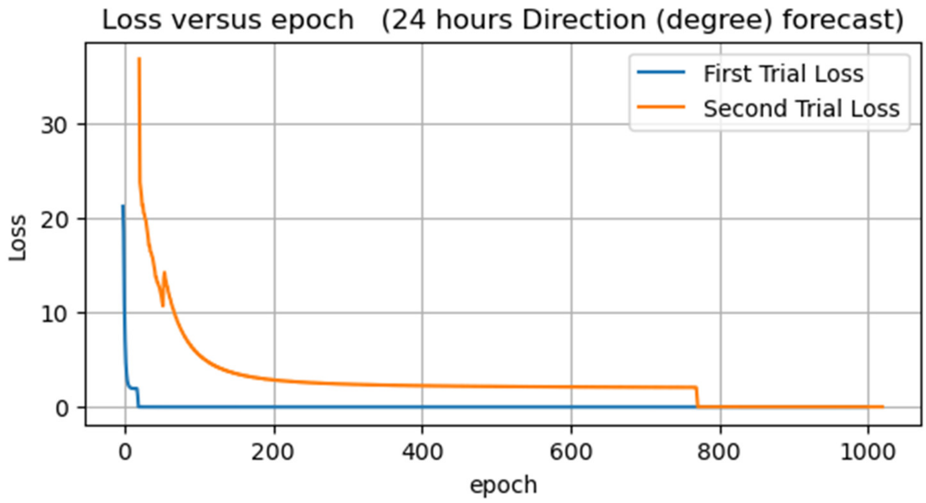

(**g**) Direction (degree) 12 hours forecast.

Figure 5. Direction forecasts of 1, 3, 6, 8, 10, 12, and 24 hours.

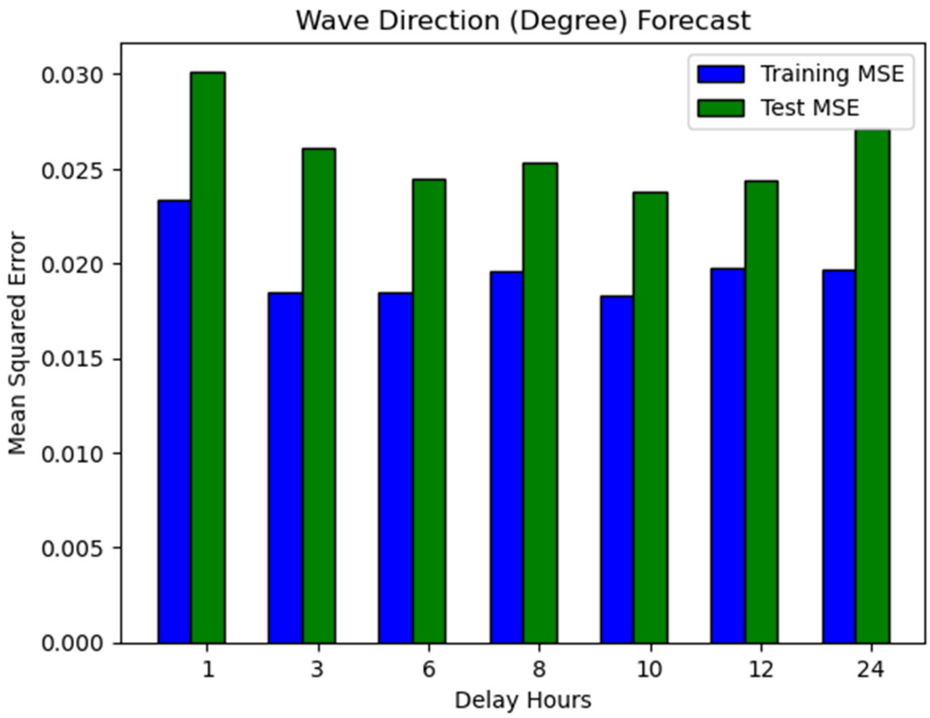

Figure 6. Training versus test MSE for wave direction forecasts in degree units.

4.3.2. Wave Direction Forecast (Radian)

The second wave direction predictions used radian units instead of the default unit degree. As part of the preprocessing of our data, the wave direction dataset in the dataframe was initially converted to a NumPy array. We then used the function numpy. radians and another dataframe were created and assigned the converted degree to radian values. This subsection analyzes the seven forecasts using the wave direction dataset in the radian unit.

Table 2 shows the experimental results of wave direction forecast in radian units, as in the previous experiments with degree units, with the next 10 hours of prediction showing the lowest MSE in both training and test situations. Moreover, in this experiment the forecasts for the next 10 hours have the lowest training and test errors. In contrast, 1 hour has the highest training and testing error.

Table 2. Direction forecast (Radian).

Direction (Radian) Forecast					
Hour	Training MSE	Test MSE	No. of Epoch	Max. trial	Elapsed Time
1	0.0469	0.0648	1000	2	16m 43s
3	0.0187	0.0249	1000	2	42m 46s
6	0.0199	0.0285	1000	2	56m 27s
8	0.0185	0.0259	1000	2	01h 08m 25s
10	0.0185	0.0245	1000	2	01h 06m 44s
12	0.0228	0.0313	1000	2	01h 50m 15s
24	0.0204	0.0261	1000	2	04h 08m 15s

Figure 8 illustrates the training and test MSEs; compared to the previous experiment result, the test MSEs are higher than training, which is quite good. The average errors for training and test are 0.0237 and 0.0322, respectively.

The learning curves of epoch versus loss are shown in Figure 7. In all seven experiments, the loss dropped to zero at some points in both the first and second trials.

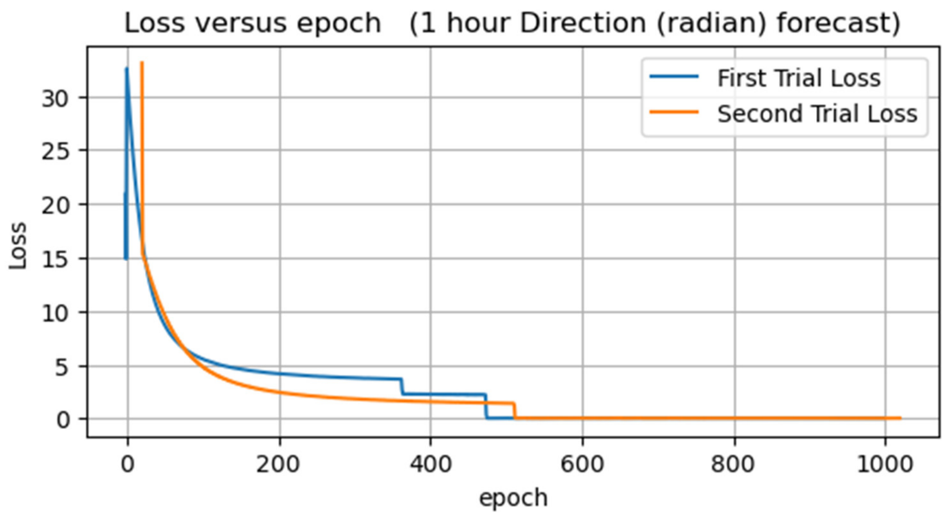

(**a**) Direction (radian) 1 hour forecast.

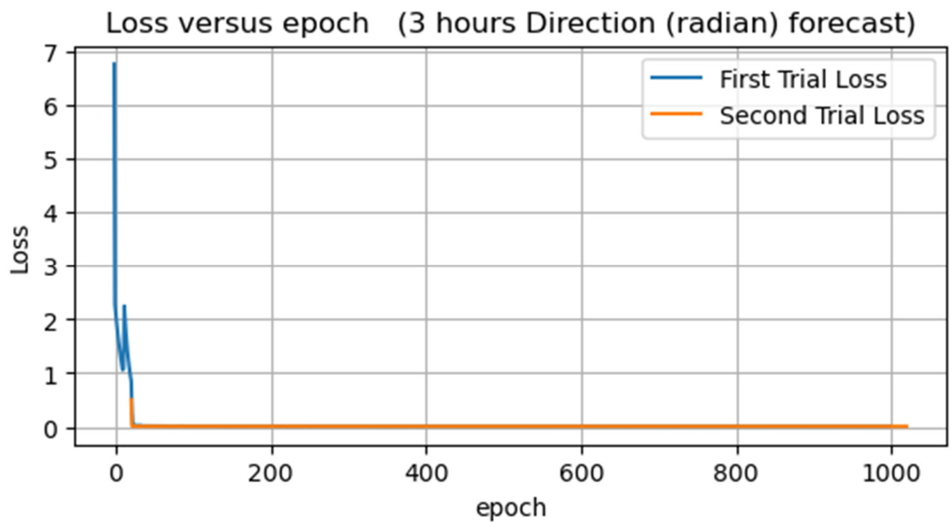

(**b**) Direction (radian) 3 hours forecast.

 doi:10.20944/preprints202304.0282.v2

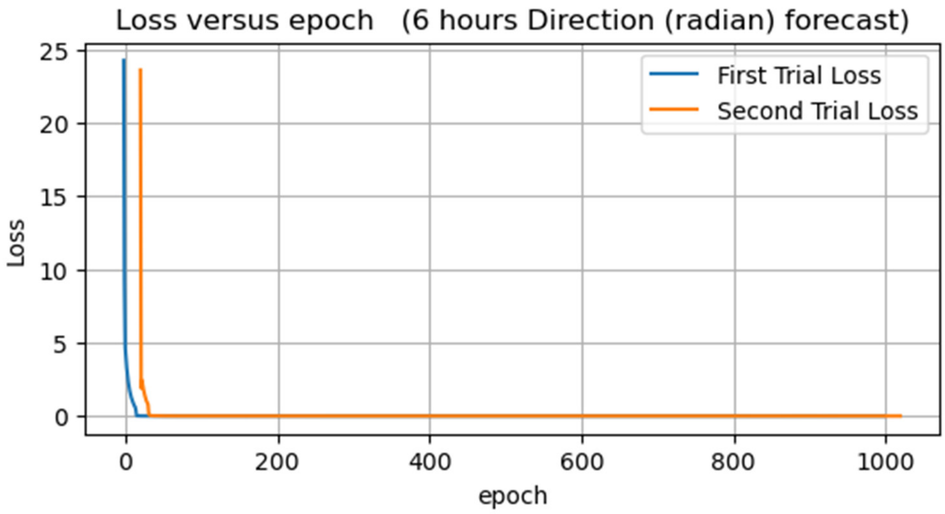

(**c**) Direction (radian) 6 hours forecast.

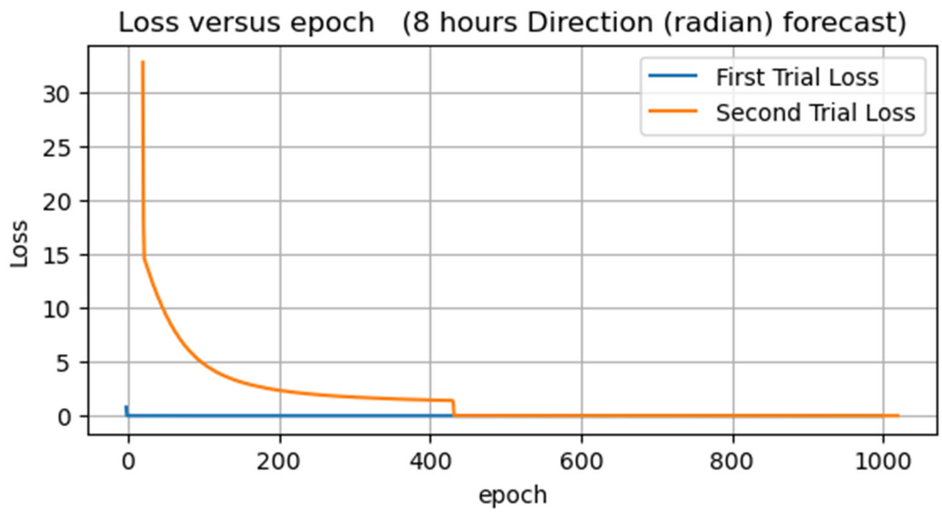

(**d**) Direction (radian) 8 hours forecast.

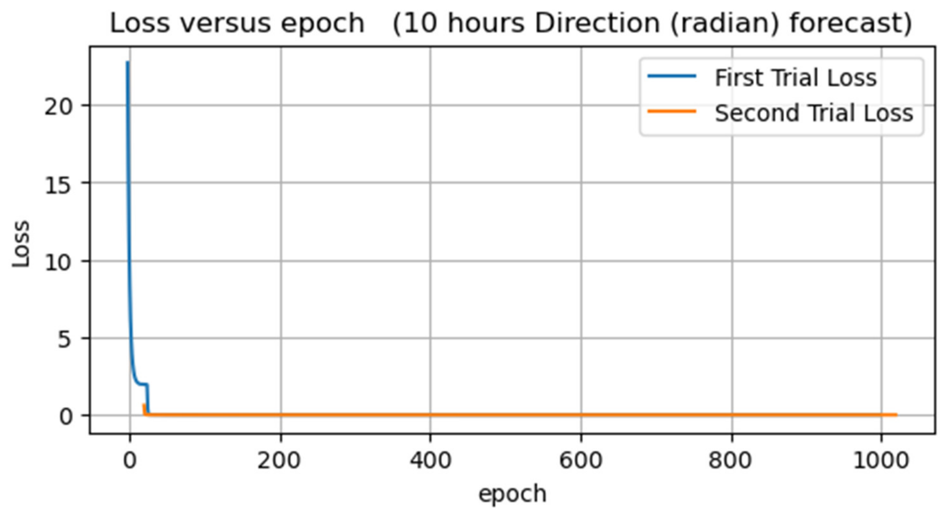

(**e**) Direction (radian) 10 hours forecast.

Preprints (www.preprints.org) | NOT PEER-REVIEWED | Posted: 18 May 2023 doi:10.20944/preprints202304.0282.v2

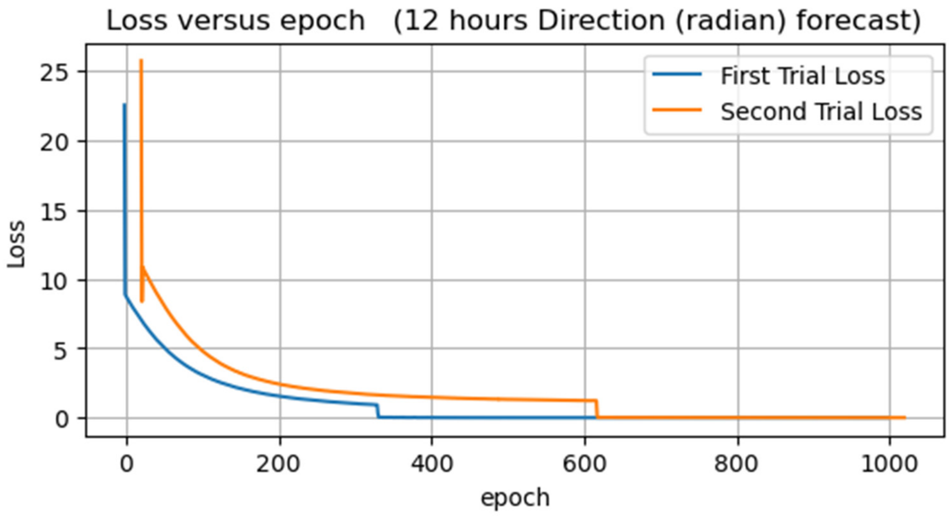

(**f**) Direction (radian) 12 hours forecast.

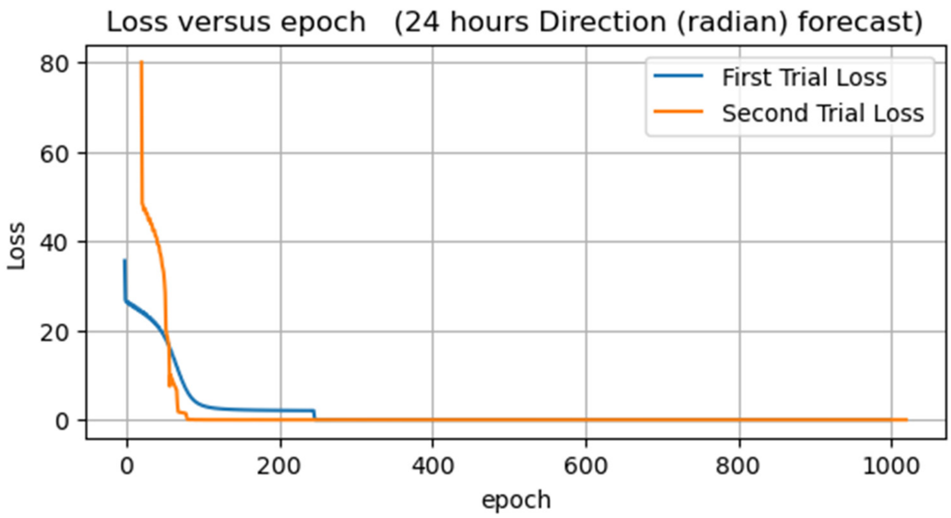

(**g**) Direction (radian) 24 hours forecast.

Figure 7. Direction forecasts of 1, 3, 6, 8, 10, 12, and 24 hours in radian units.

Preprints (www.preprints.org) | NOT PEER-REVIEWED | Posted: 18 May 2023 doi:10.20944/preprints202304.0282.v2

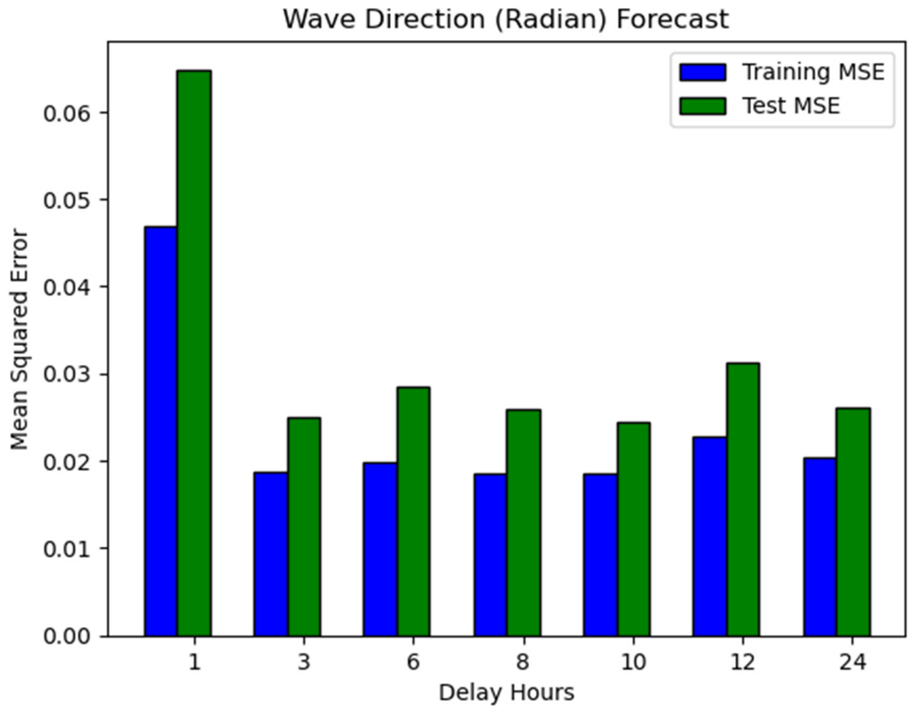

Figure 8. Training versus test MSE for wave direction forecasts in radian units.

4.3.3. Comparison of Wave Direction Forecast in Degree and Radian Units

The main objective of using two different direction units is to find the one with the least forecast error. When forecasting wave direction in both units of measure, the epoch loss will eventually be zero. The forecast for the next 10 hours has the lowest training and testing errors in both units. For an 8-hours forecast in a degree unit, the training and test MSE is much higher than for a radiant unit. For the remaining experiments, the errors of forecast in degree units are slightly lower. When comparing forecast in two different units, the training and test errors are very close because the error margins in the corresponding forecast hours are minimal. As can be seen from Tables 1 and 2, the 24-hour forecasts in radian units are more expensive than the forecasts in degree units.

4.3.4 Wave Speed Forecast

The wave speed was measured in it is default unit (ms^{-1}). This subsection analyzes the seven forecast experiments using the wave speed dataset.

Table 3 shows the experimental results of wave speed forecasts. The forecast of wave speed for 8 and 24 hours has the lowest training MSE of 0.0027, while the forecast for the next 1 hour has the highest training MSE. Conversely, the forecast for 3 and 12 hours has the lowest and highest test MSE, respectively. The learning curves are shown in Figure 9. In each of the seven experiments, the loss dropped to zero at some point.

Table 3. Speed forecast.

Speed Forecast (m/s)					
Hour	Training MSE	Test MSE	No. of Epoch	Max. trial	Elapsed Time
1	0.0036	0.0083	1000	2	20m 32s
3	0.0033	0.0058	1000	2	39m 24s
6	0.0034	0.0448	1000	2	01h 08m 34s
8	0.0027	0.0154	1000	2	01h 22m 35s
10	0.0035	0.0046	1000	2	01h 48m 49s
12	0.0029	0.0625	1000	2	02h 08m 59s

 doi:10.20944/preprints202304.0282.v2

24	0.0027	0.0513	1000	2	05h 12m 45s

Figure 10 shows the training and test MSEs. The graph shows that the test MSEs are higher than the training MSEs in all seven-speed forecast experiments, which is similar to the two previous experiments in Figures 5 and 7, which followed the same pattern. The data set was shuffled in each experiment to allow the models to learn perfectly and avoid sampling bias.

However, when we compared the training and test MSEs of forecasting wave speed and direction in two different units of measurement, the former had the least forecast errors when compared with the latter. As for the running cost, the elapsed time for the 24-hour speed forecast is higher than the others, as shown in Table 3.

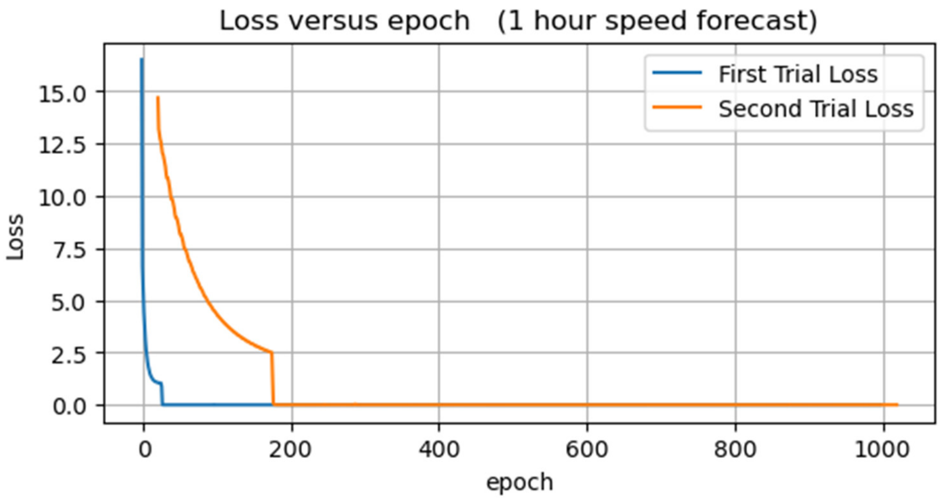

(**a**) Speed 1 hour forecast.

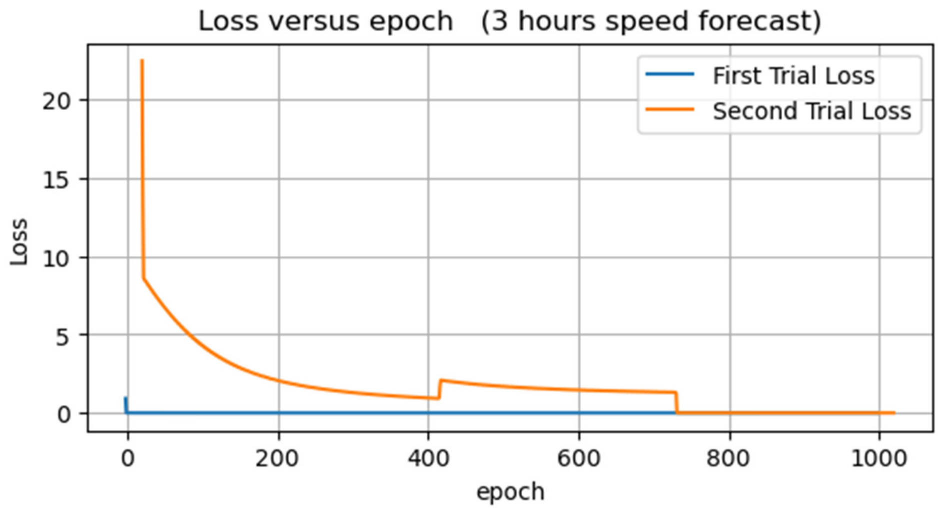

(**b**) Speed 3 hours forecast.

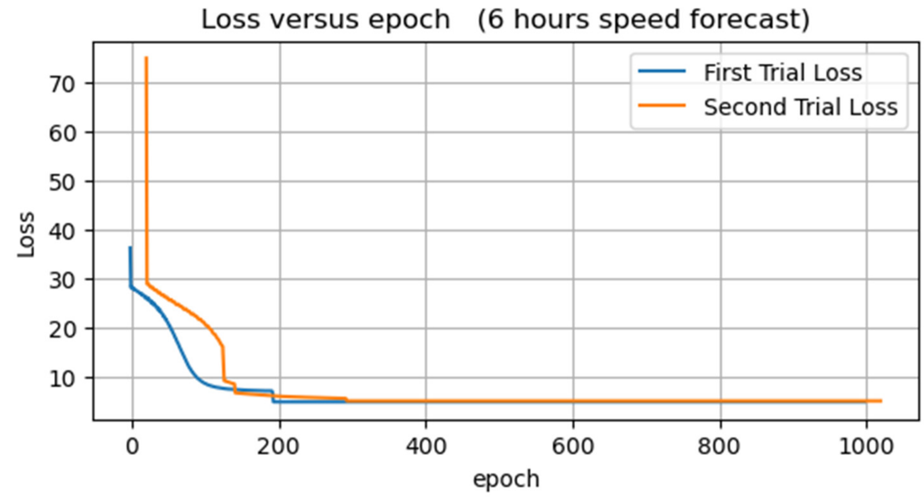

(**c**) Speed 6 hours forecast.

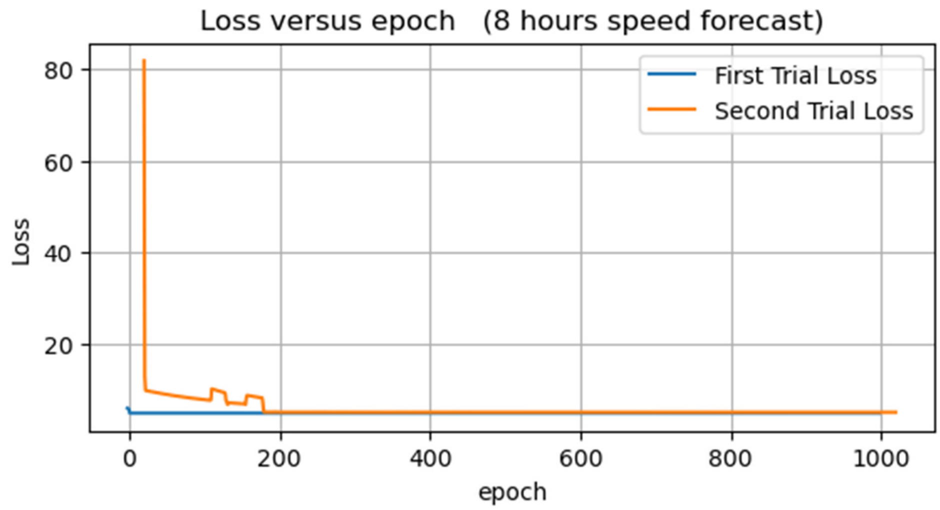

(**d**) Speed 8 hours forecast.

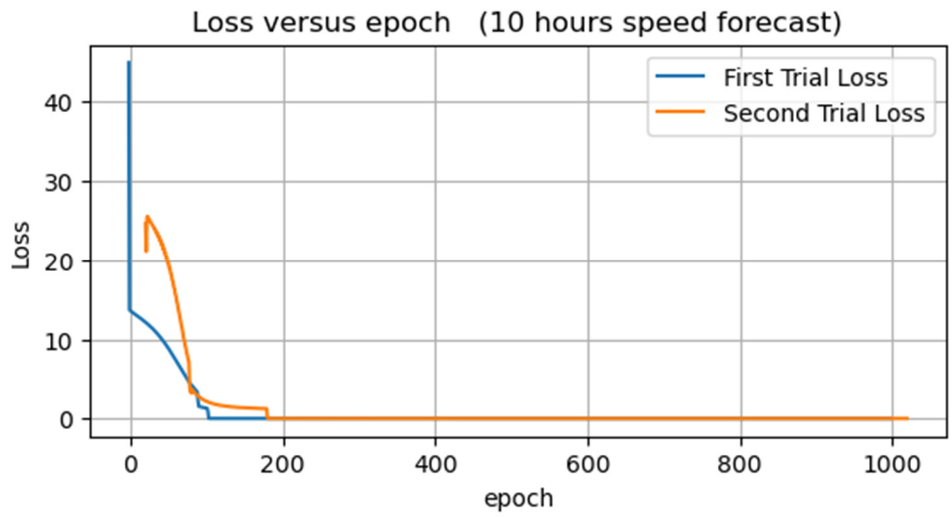

(**e**) Speed 10 hours forecast.

Preprints (www.preprints.org) | NOT PEER-REVIEWED | Posted: 18 May 2023 doi:10.20944/preprints202304.0282.v2

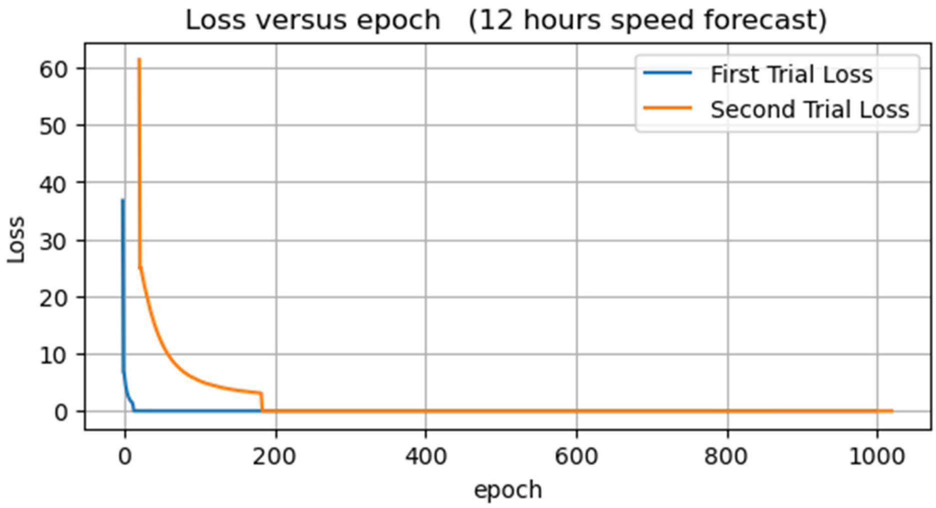

(**f**) Speed 12 hours forecast.

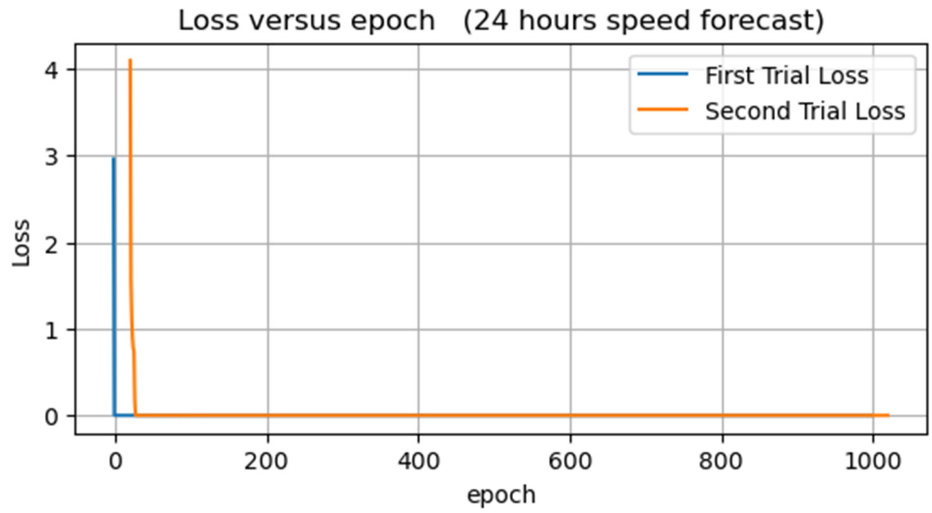

(**g**) Speed 24 hours forecast.

Figure 9. Speed forecast of 1, 3, 6, 8, 10, 12, and 24 hours.

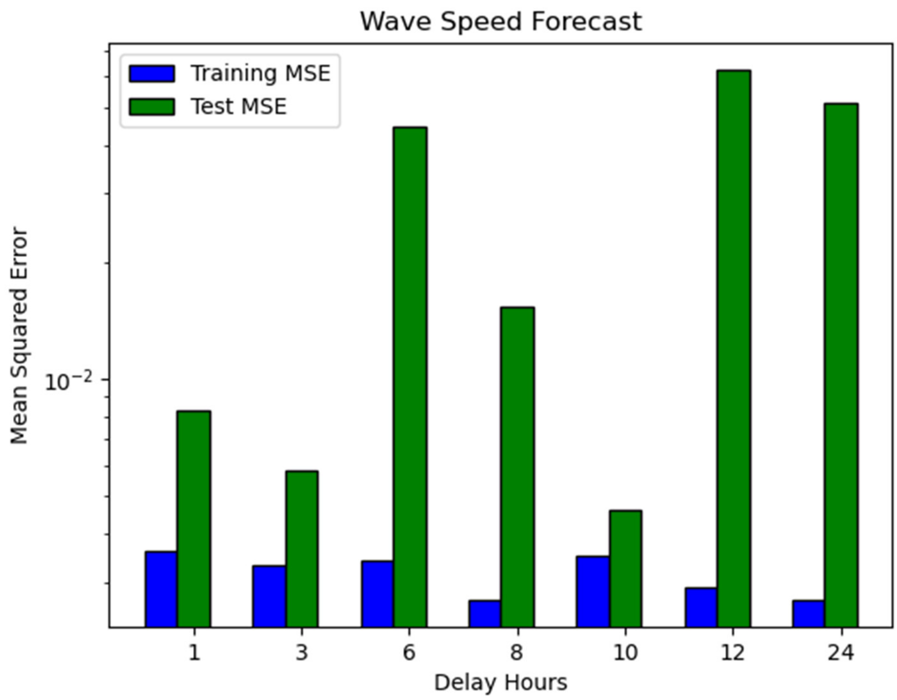

Figure 10. Training versus test MSE for wave speed predictions.

4.4. Comparative Analysis of Time Series Forecasting Models

To validate the performance of the proposed model, we used the study dataset, and air quality index dataset and ran two comparative experiments with other time series forecasting algorithms. We used five lookbacks for each experiment. Figures 11 and 12 comprise the comparative analysis of wave speed and direction forecast respectively.

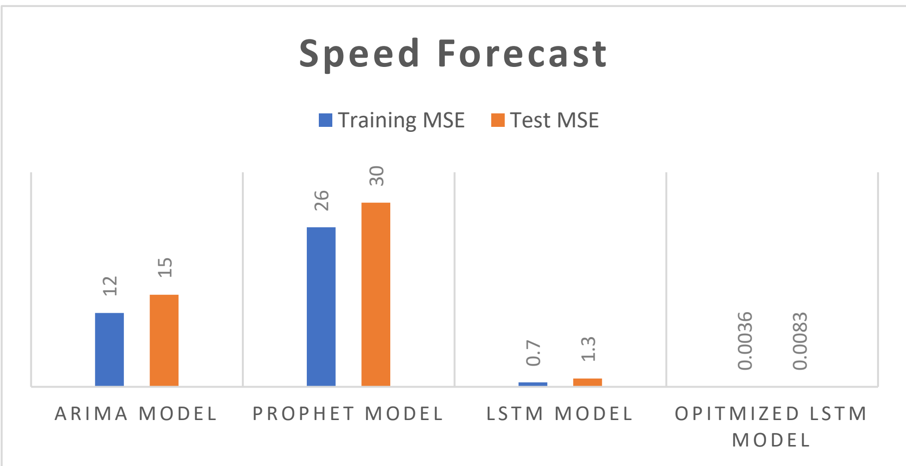

Figure 11. Comparative analysis of time-series forecast models for wave speed.

Preprints (www.preprints.org) | NOT PEER-REVIEWED | Posted: 18 May 2023 doi:10.20944/preprints202304.0282.v2

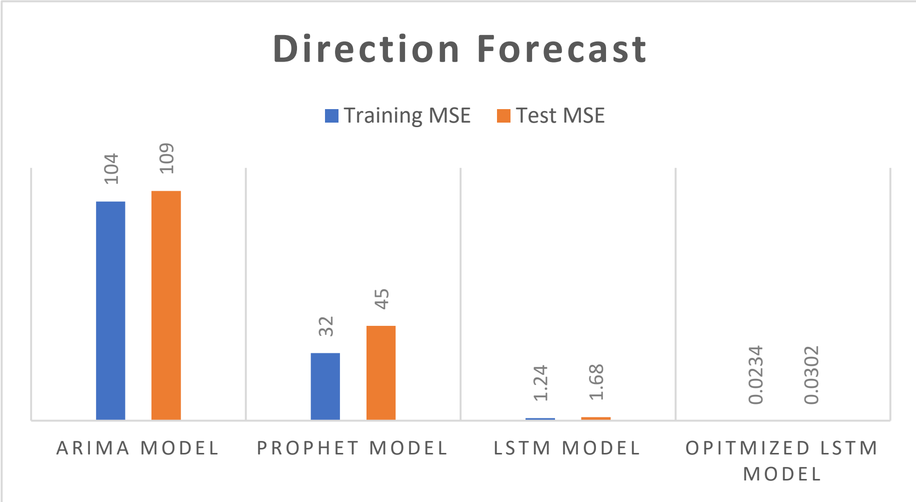

Figure 12. Comparative analysis of time-series forecast models for wave direction.

The results of the comparative analysis from the above figures show that the newly proposed model outperforms the other time series forecasting models.

Figure 13 illustrates the comparative analysis of time-series forecast models for the air quality index. The optimized LSTM (proposed model) outperformed other models. The two experiments' results showed that the optimized LSTM performed better than the other models.

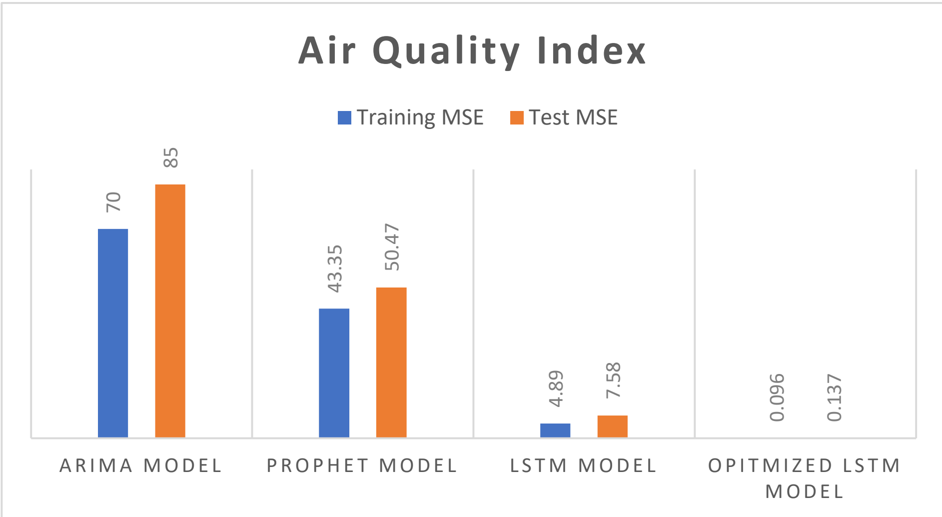

Figure 13. Comparative analysis of time-series forecast models for air quality index.

5. Future Research Direction

The wave equation we used to model ocean wave speed in numerical simulations may need to be revised to capture ocean waves' complex behavior accurately. In the future, we will use higher-order partial differential equations that can solve complex system problems more accurately. The optimized LSTM models proposed in this study were developed using univariate time series techniques, which limit the forecast of wave conditions to only one element or feature at a time. As part of the feasibility and evaluation of marine energy harvesting, we plan to use advanced multivariate time series forecasting and optimization techniques in our future research. In addition, the data we used includes only 4925 data points. In our future study, we plan to collect more data from two or more stations, which could be three or four times the current dataset.

 doi:10.20944/preprints202304.0282.v2

6. Conclusions

This research used two numerical methods to model and simulate the wave speed and direction with sample data. We presented a novel univariate time series forecasting models, and make forecast for wave speed and direction. We found that the wave speed forecast had less error than direction during the experiment. The forecast of wave direction was performed using two different units of measurement. The forecast in degrees has less error than that in radians. However, the former is slightly less expensive to run when compared to the latter for the 24-hour forecast, despite the differences in prediction in the two units. The error margins and the time difference of the corresponding hours clearly show that each unit's forecast can generate less errors. However, the speed forecast is more expensive to run compared to direction. Our proposed model incorporates the robust LSTM network with the effective hyperparameter tuning optimization technique and creates a novel and promising approach for univariate time series forecasting.

The proposed model's extraordinary performance against three time-series forecasting models highlights its potential for practical application in Dynamic Ocean forecasting, sustainable port management and other fields such as finance, energy, etc.

Author Contributions: Writing—original draft preparation, Z.K.Lawal and A.C.Idris.; writing—review and editing, Z.K.L.awal, A.C.Idris., H.Yassin and D.T.C.Lai.; supervision, A.C.Idris., H.Yassin. and D.T.C.Lai.; funding acquisition, H.Yassin. and A.C.Idris .Conducting experiments Z.K.Lawal, supervision, A.C.Idris., H.Yassin. and D.T.C.Lai. All authors have read and agreed to the published version of the manuscript.

Funding: This work is funded by Universiti Brunei Darussalam, Brunei under Grant ref: UBD/RSCH/1.11/FICBF(b)/2020/004.

Data Availability Statement: The ADCP data are not publicly available because it belongs to the Universiti Brunei Darussalam. The Air Quality Index dataset used for validation is publically available on Kaggle Website.

Conflicts of Interest: The authors declare no conflict of interest**.**

References

1. Uihlein, A.; Magagna, D. Wave and tidal current energy—A review of the current state of research beyond technology. *Renew. Sustain. Energy Rev.* **2016**, *58*, 1070–1081. https://doi.org/10.1016/j.rser.2015.12.284.
2. M. Alif, R. Yonanta, A. R. #1, A. #2, and N. Subasita, "Wind Wave Prediction by using Autoregressive Integrated Moving Average model : Case Study in Jakarta Bay". https://doi.org/10.21108/indojc.2018.42.300.
3. Institute of Electrical and Electronics Engineers. Indonesia Section, IEEE Signal Processing Society. Indonesia Chapter, Universitas Telkom, Multimedia University, Universitas Gadjah Mada, and Institute of Electrical and Electronics Engineers. In Proceedings of the 8th International Conference on Information and Communication Technology (ICoICT), Yogyakarta, Indonesia, 24–26 June 2020. Available online: https://doi.org/10.1109/ICoICT49345.2020.9166297 (accessed on 1 November 2022).
4. Durán-Rosal, A.; Fernández, J.; Gutiérrez, P.; Hervás-Martínez, C. Detection and prediction of segments containing extreme significant wave heights. *Ocean Eng.* **2017**, *142*, 268–279. https://doi.org/10.1016/j.oceaneng.2017.07.009.
5. Bai, G.; Wang, Z.; Zhu, X.; Feng, Y. Development of a 2-D deep learning regional wave field forecast model based on convolutional neural network and the application in South China Sea. *Appl. Ocean Res.* **2021**, *118*. https://doi.org/10.1016/j.apor.2021.103012.
6. Song, T.; Han, R.; Meng, F.; Wang, J.; Wei, W.; Peng, S. A significant wave height prediction method based on deep learning combining the correlation between wind and wind waves. *Front. Mar. Sci.* **2022**, *9*. https://doi.org/10.3389/fmars.2022.983007.
7. slam, M.; Zaman, H.; Jahra, F. Investigation of Numerical Modelling Techniques for Predicting Highly Nonlinear Extreme Waves in Shallow and Deep Water. In Proceedings of the Oceans Conference Record (IEEE), 2021; Volume 2021-September. https://doi.org/10.23919/OCEANS44145.2021.9705943.
8. Kim, J.; Kim, T.; Yoo, J.; Ryu, J.-G.; Do, K.; Kim, J. STG-OceanWaveNet: Spatio-temporal geographic information guided ocean wave prediction network. *Ocean Eng.* **2022**, *257*. https://doi.org/10.1016/j.oceaneng.2022.111576.

9. T. F. Duda et al. Issues and progress in the prediction of ocean submesoscale features and internal waves. In Proceedings of the 2014 Oceans - St. John's, OCEANS 2014, January 2015. https://doi.org/10.1109/OCEANS.2014.7003282.
10. Marine Technology Society, American Society of Civil Engineers., and Institute of Electrical and Electronics Engineers. Oceans '97 MTS/IEEE: Conference proceedings, World Trade and Convention Centre, Halifax, Nova Scotia, Canada. Oceans '96 MTS/IEEE Conference Committee, 6–9 October 1997.
11. Y. Li *et al.* Numerical Simulations for Lithium-Ion Battery Pack Cooled by Different Minichannel Cold Plate Arrangements. *Int. J. Energy Res.* **2023**, *2023*, 1–18. https://doi.org/10.1155/2023/8207527.
12. V. G. Panchang, B. Xu, and Z. Demirbilek, Wave Prediction Models for Coastal Engineering Applications.
13. Zheng, K.; Sun, J.; Guan, C.; Shao, W. Analysis of the Global Swell and Wind Sea Energy Distribution Using WAVEWATCH III. *Adv. Meteorol.* **2016**, *2016*. https://doi.org/10.1155/2016/8419580.
14. N. Booij, R. C. Ris, and L. H. Holthuijsen, A third-generation wave model for coastal regions 1. Model description and validation. 1999.
15. H. L. Tolman, User manual and system documentation of WAVEWATCH III TM version 3.14 †. 2009.
16. WAVEWATCH III Model Description.
17. Wei, J.; Malanotte-Rizzoli, P.; Eltahir, E.A.B.; Xue, P.; Xu, D. Coupling of a regional atmospheric model (RegCM3) and a regional oceanic model (FVCOM) over the maritime continent. *Clim. Dyn.* **2014**, *43*, 1575–1594. https://doi.org/10.1007/s00382-013-1986-3.
18. Alghamdi, H.; Maduabuchi, C.; Albaker, A.; Almalaq, A.; Alsuwian, T.; Alatawi, I. Machine Learning Performance Prediction of a Solar Photovoltaic-Thermoelectric System with Various Crystalline Silicon Cell Types. *Int. J. Energy Res.* **2023**, *2023*, 1–26. https://doi.org/10.1155/2023/1990593.
19. Song, T.; Jiang, J.; Li, W.; Xu, D. A Deep Learning Method with Merged LSTM Neural Networks for SSHA Prediction. *IEEE J. Sel. Top. Appl. Earth Obs. Remote. Sens.* **2020**, *13*, 2853–2860. https://doi.org/10.1109/JSTARS.2020.2998461.
20. Bellotti, G. A modal decomposition method for the analysis of long waves amplification at coastal areas. *Coast. Eng.* **2019**, *157*. https://doi.org/10.1016/j.coastaleng.2019.103632.
21. Cavaleri, L.; Abdalla, S.; Benetazzo, A.; Bertotti, L.; Bidlot, J.-R.; Breivik, Ø.; Carniel, S.; Jensen, R.E.; Portilla-Yandun, J.; Rogers, W.E.; et al. Wave modelling in coastal and inner seas. *Prog. Oceanogr.* **2018**, *167*, 164–233. https://doi.org/10.1016/j.pocean.2018.03.010.
22. Huang, L.; Jing, Y.; Chen, H.; Zhang, L.; Liu, Y. A regional wind wave prediction surrogate model based on CNN deep learning network. *Appl. Ocean Res.* **2022**, *126*. https://doi.org/10.1016/j.apor.2022.103287.
23. Berbić, J.; Ocvirk, E.; Carević, D.; Lončar, G. Application of neural networks and support vector machine for significant wave height prediction. *Oceanologia* **2017**, *59*, 331–349. https://doi.org/10.1016/j.oceano.2017.03.007.
24. Zanuttigh, B.; Formentin, S.M.; Briganti, R. A neural network for the prediction of wave reflection from coastal and harbor structures. *Coast. Eng.* **2013**, *80*, 49–67. https://doi.org/10.1016/j.coastaleng.2013.05.004.
25. Elbisy, M.S. Sea Wave Parameters Prediction by Support Vector Machine Using a Genetic Algorithm. *J. Coast. Res.* **2015**, *31*, 892–899. https://doi.org/10.2112/JCOASTRES-D-13-00087.1.
26. Wang, J.; Chen, Z.; Zhang, F. A Review of the Optimization Design and Control for Ocean Wave Power Generation Systems. *Energies* **2021**, *15*. https://doi.org/10.3390/en15010102.
27. Rafeal, W. Energy from Ocean Waves. 2008.
28. Ocean Wave Energy Harvesting 4.1 Introduction to Ocean Wave Energy Harvesting. 2010. Available online: https://edisciplinas.usp.br/pluginfile.php/5534592/mod_resource/content/1/25.Chapter%204.%20Ocean%20Wave%20Energy%20Harvesting.pdf (accessed on 24 October 2022).
29. Khan, M.Z.A.; Khan, H.A.; Aziz, M. Harvesting Energy from Ocean: Technologies and Perspectives. *Energies* **2022**, *15*. https://doi.org/10.3390/en15093456.
30. Deshmukh, A.N.; Deo, M.C.; Bhaskaran, P.K.; Nair, T.M.B.; Sandhya, K.G. Neural-Network-Based Data Assimilation to Improve Numerical Ocean Wave Forecast. *IEEE J. Ocean. Eng.* **2016**, *41*, 944–953. https://doi.org/10.1109/JOE.2016.2521222.
31. Cardone, V.; Greenwood, J. Ocean Surface Wave Prediction - Current Trends and Future Prospects. In *Oceans Conference Record (IEEE)*; 1986; pp. 1372–1378. https://doi.org/10.1109/oceans.1986.1160315.
32. Brunei Darussalam (2012) Climate Technology Centre & Network Tue, 07_18_2017. Available online: https://www.ctc-n.org/content/brunei-darussalam-2012 (accessed on 25 November 2022).

33. Petris, G.; Cianferra, M.; Armenio, V. A numerical method for the solution of the three-dimensional acoustic wave equation in a marine environment considering complex sources. *Ocean Eng.* **2022**, *256*. https://doi.org/10.1016/j.oceaneng.2022.111459.
34. Ozgun, O.; Kuzuoglu, M. Physics-based modeling of sea clutter phenomenon by a full-wave numerical solver. *Wave Motion* **2022**, *109*. https://doi.org/10.1016/j.wavemoti.2021.102872.
35. Oyedeji, M.O.; AlDhaifallah, M.; Rezk, H.; Mohamed, A.A.A. Computational Models for Forecasting Electric Vehicle Energy Demand. *Int. J. Energy Res.* **2023**, *2023*, 1–16. https://doi.org/10.1155/2023/1934188.
36. Tang, T.; Adcock, T.A. The influence of finite depth on the evolution of extreme wave statistics in numerical wave tanks. *Coast. Eng.* **2021**, *166*. https://doi.org/10.1016/j.coastaleng.2021.103870.
37. Zhou, H.; Hu, K.; Mao, L.; Sun, M.; Cao, J. Research on planing motion and stability of amphibious aircraft in waves based on cartesian grid finite difference method. *Ocean Eng.* **2023**, *272*. https://doi.org/10.1016/j.oceaneng.2023.113848.
38. Varela, J.; Rodriguez, G.; Soares, C.G. Comparison study between the Fourier and the Hartley transforms for the real-time simulation of the sea surface elevation. *Appl. Ocean Res.* **2018**, *74*, 227–236. https://doi.org/10.1016/j.apor.2018.03.002.
39. Agarwal, S.; Sriram, V.; Liu, P.-F.; Murali, K. Waves in waterways generated by moving pressure field in Boussinesq equations using unstructured finite element model. *Ocean Eng.* **2022**, *262*. https://doi.org/10.1016/j.oceaneng.2022.112202.
40. Katsaounos, C.Z.; Giokas, D.L.; Leonardos, I.D.; Karayannis, M.I. Speciation of phosphorus fractionation in river sediments by explanatory data analysis. *Water Res.* **2007**, *41*, 406–418. https://doi.org/10.1016/j.watres.2006.10.028.
41. Uğurlu, B.; Kahraman, I.; Soares, C.G. Numerical investigation of the Fourier–Kochin theory for wave-induced response estimation of floating structures. *Ocean Eng.* **2022**, *247*. https://doi.org/10.1016/j.oceaneng.2022.110562.
42. Hochreiter, S.; Schmidhuber, J.U. Long Short-Term Memory.
43. Liu, D.; Wei, A. Regulated LSTM Artificial Neural Networks for Option Risks. *Fintech* **2022**, *1*, 180–190. https://doi.org/10.3390/fintech1020014.
44. Zhu, Y.; Hu, Z.; Yuan, S.; Zheng, J.; Lu, D.; Huang, F. Raindrop Size Distribution Prediction by an Improved Long Short-Term Memory Network. *Remote. Sens.* **2022**, *14*. https://doi.org/10.3390/rs14194994.
45. Gautam, S.; Henry, A.; Zuhair, M.; Rashid, M.; Javed, A.R.; Maddikunta, P.K.R. A Composite Approach of Intrusion Detection Systems: Hybrid RNN and Correlation-Based Feature Optimization. *Electronics* **2022**, *11*. https://doi.org/10.3390/electronics11213529.
46. F. A. Gers, J. Schmidhuber, and F. Cummins, Learning *to* Forget: Continual Prediction with LSTM. Available online: http://m.idsia.ch/.
47. Van Houdt, G.; Mosquera, C.; Nápoles, G. A review on the long short-term memory model. *Artif. Intell. Rev.* **2020**, *53*, 5929–5955. https://doi.org/10.1007/s10462-020-09838-1.
48. Stateczny, A.; Bolugallu, S.M.; Divakarachari, P.B.; Ganesan, K.; Muthu, J.R. Multiplicative Long Short-Term Memory with Improved Mayfly Optimization for LULC Classification. *Remote. Sens.* **2022**, *14*. https://doi.org/10.3390/rs14194837.
49. Graves, A.; Schmidhuber, J. Framewise phoneme classification with bidirectional LSTM and other neural network architectures. *Neural Netw.* **2005**, *18*, 602–610. https://doi.org/10.1016/j.neunet.2005.06.042.
50. Ge, S.; Su, W.; Gu, H.; Rauste, Y.; Praks, J.; Antropov, O. Improved LSTM Model for Boreal Forest Height Mapping Using Sentinel-1 Time Series. *Remote. Sens.* **2022**, *14*, 5560. https://doi.org/10.3390/rs14215560.
51. Zhang, L.; Cai, Y.; Huang, H.; Li, A.; Yang, L.; Zhou, C. A CNN-LSTM Model for Soil Organic Carbon Content Prediction with Long Time Series of MODIS-Based Phenological Variables. *Remote. Sens.* **2022**, *14*. https://doi.org/10.3390/rs14184441.
52. Pham, H. A New Criterion for Model Selection. *Mathematics* **2019**, *7*. https://doi.org/10.3390/MATH7121215.